

Microphase Separation of PS-*b*-PMMA Block Copolymer and Hard Mask Formation on Graphene

Hande Yöndemli¹, Cian Cummins², Mustafa Ersöz³, Michael A. Morris⁴

¹Selcuk University, Advanced Technology Research & Application Center
Konya, Turkey

handeyondemli@gmail.com

²Universite de Bordeaux

Bordeaux, France

cian.a.cummins@gmail.com

³Selcuk University, Department of Chemistry, Konya, Turkey

ersozm@gmail.com

⁴Trinity College Dublin, Dublin, Ireland

morrism2@tcd.ie

Abstract - In this paper, we studied microphase separation on and pattern transfer to graphene substrates using commercially obtained poly(styrene)-*block*-poly(methyl methacrylate) (PS-*b*-PMMA) block copolymers (BCP) possessing lamellar and cylindrical morphologies. Self-assembly was achieved using a thermal annealing technique, and well-arranged microphase separated patterns were obtained. Insertion of alumina oxide into the patterns followed by etch treatments allowed pattern transfer to the substrate surface. After pre-studies were carried out and parameters were optimized on SiO₂ coated Si surfaces, experiments were continued on SiO₂ coated graphene surfaces. Characterization was performed mainly by atomic force microscope (AFM) for observing microphase separated patterns and etching effects. This study provides further application of block copolymers on new materials for semiconductor and other potential technological (*e.g.* sensor, energy storage) applications.

Keywords: AFM, block copolymers, microphase separation, nanowire, self-assembly

1. Introduction

Moore's law has been the driver for miniturization of electronic device elements since the 1960's [1]. As scaling advancements have slowed (due to diffraction limits), alternative patterning options are being explored. In particular, block copolymers (BCPs) are being investigated extensively for dimensional scaling. There are numerous reviews of BCPs and their uses [2], [3], [4]. BCPs are being used in many fields, notably as membranes, photonic crystals, electronic devices due to their ability to be patterned over large areas with controllable dimensions. By means of self-assembly of block copolymer films, promising developments have been made for the silicon microelectronics industry in recent years [5]. Broad information regarding the subject is present in the literature [6].

Graphene, is a promising material for applications in the electronics industry. After the Nobel prize winning discovery of Geim and Novoselov, graphene is a major candidate to be used in the semiconductor industry due to its superior properties such as thermal [7] and electrical [8] conductivity, mechanical strength [9], ... *etc.* Being a single-layered material, it is composed of sp² hybrid carbons, having hexagonal geometry. Since a graphene layer is one-atom thick structure, it is described as a 2D material. Graphene is a very flexible material with a high specific surface area. However, contrary to all these advantages, graphene's lack of an usable band gap causes a serious problem for potential applications in the semi-conductor industry. Thus, its band gap needs to be tailored [10]. Studies related to this issue have been conducted [11]. Recently, directed self assembly (DSA) of BCPs on graphene chemical patterns has been studied [11] and the results are of great importance for the future integration of graphene in the electronics industry. It is known that graphene nanoarrays show semi-conducting properties with a maximum band gap of 1.3 eV [12].

With the aim of gaining optimum band gap in graphene, there is a clear need to control the graphene geometry is required. In order to make these changes, nanopatterning techniques have been used. In order to integrate these patterned

materials into device manufacture, industry compatible methods are necessary, and here, we demonstrate the feasibility of using BCP patterning towards graphene device fabrication.

Figure 1 displays the process flow employed in this work. The graphene layer which was synthesized by chemical vapor deposition (CVD) technique on Cu foil (Figure 1a) was transferred onto SiO₂ coated Si (Si/SiO₂) (Figure 1b) layer. PS-*b*-PMMA BCP solutions were coated on the graphene layer. After the annealing processes, highly ordered microphase separation was obtained. First a template was developed by selective etching of one of the blocks forming the phase-separated BCP structure. This template acts as a mask for the transfer of the pattern to the underlayer [13]. A metal salt inclusion technique was used to increase etch resistance of the PS pattern. In the following step, the as-formed aluminium oxide based hard mask was etched, and, thus, graphene nanoarrays were formed.

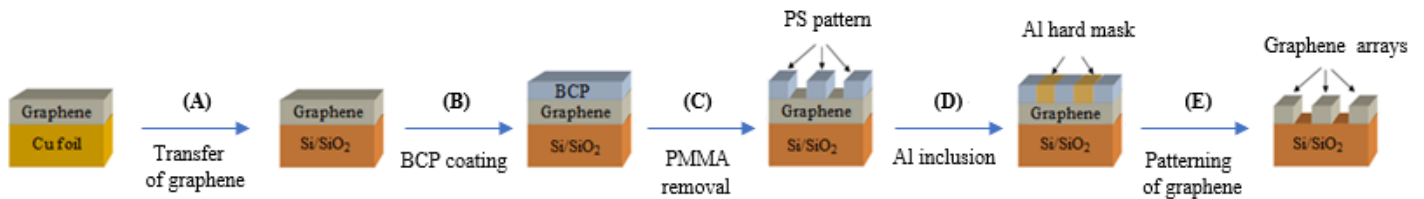


Fig. 1: Applied procedure in order to obtain graphene nanoarrays.

The band gap of graphene nanoarrays obtained after the etching steps is directly related to the molecular weights of BCPs used at the initial step. Because of this reason, in order to reach smaller dimensions and to increase sensitivity, blocks with smaller molecular weights are preferred. Graphene obtained as the result of all these processes will possess a band-gap optimized structure and hence, carry promising physical properties for semi-conductor industry applications. The aim of this study is to modify graphene chemistry and improve its electrical properties with the help of the DSA technique.

2. Materials and Method

Graphene layers were coated on Si/SiO₂ wafers by a CVD technique at 1000°C under 50mTorr pressure using ethanol vapor as the carbon source, and Cu foil as the catalyst. 39.5kD-17.7kD poly(styrene)-*block*-poly(methacrylate) (referred to as PS-*b*-PMMA) BCP was supplied from ARKEMA, France, PS-OH brush and 37kD-37kD PS-*b*-PMMA BCP were supplied from Polymer Source Inc., Canada and were used as received. Brush and 37kD-37kD BCP solutions were prepared as 1% (w/w) in toluene (Sigma Aldrich), 39kD-17.7kD BCP solutions were prepared as 1.5 (w/w) in toluene. All of the solutions were coated onto graphene layers at 3200 rpm for 30 seconds.

2.1. Microphase Separation using 37kD-37kD and 39.5 kD-17.7 kD PS-*b*-PMMA on Si Substrates

Linear (50% PS) brush coated samples were kept in a vacuum oven at 170°C for about 2 hours in order to modify surface chemistry. The PS brush modification enables perpendicular orientation of lamellar features to the substrate surface, after spin coating of the 37kD-37kD PS-*b*-PMMA BCP, and annealing at 240°C for 20 minutes on a hot plate, AFM results show the highly ordered lamellar pattern obtained in Figure 2a and b.

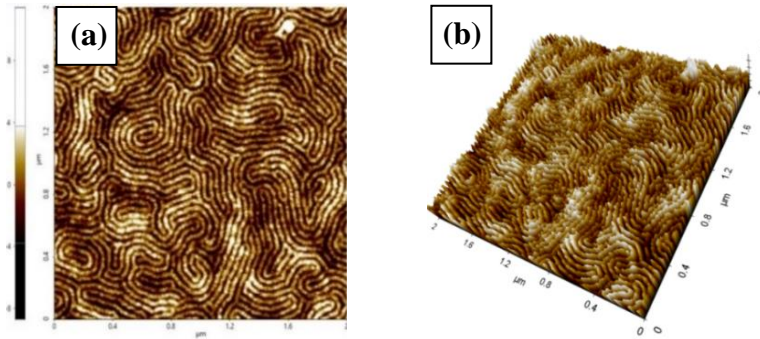


Fig. 2: (a) 1D and (b) 3D AFM images of surfaces coated and thermally annealed with 70% PS brush for 2 hours at 170°C, and coated with 37kD-37kD PS-*b*-PMMA and heated on hot plate at 240°C for 20 minutes, followed by 4-minute wet etching with acetic acid.

On the other hand, cylindrical PS-OH brush coated sample was kept at 190°C, and after coating with 39.5kD-17.7kD, hot plate annealing was done at 230°C. As shown in Figure 3, a perpendicular cylindrical pattern results after self-assembly. A sample line profile is given in Figure 3.

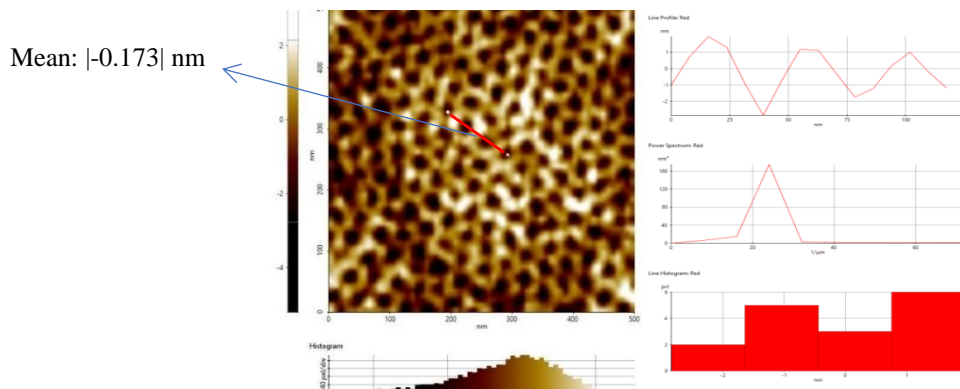


Fig. 3: AFM profile of the surface coated and thermally annealed with PS-OH brush for 2 hours at 190°C, coated with 39.5kD-17.7kD PS-*b*-PMMA and heated on hot plate at 230°C for 20 minutes, followed by 3-minute wet etching with acetic acid.

Table 1 shows the line profile values of substrates coated with PS-OH brush and 39.5kD-17.7kD BCP, and subsequently wet etched using acetic acid between 1-10 minutes. It was observed that 3-4 minutes of interaction was optimum based on the resolution of the AFM images which indicated good order and maximum contrast in the pattern. A more quantitative study was carried out by measuring line profiles across the hexagonal pattern. This proved inconclusive except showing that the process is complex. Results are shown in Table 1. We believe that the variation data shows that much of the PMMA is etched in a very short time (1 min). However, the line profile differences then begin to decrease due either swelling or a reaction with the PS. 5 mins represents the onset of acid induced damage to the film. After this, the structural regularity begins to decrease as the damage increases leaving a highly roughened film as shown by the profiles.

Table 1: Line profile values of substrates coated with PS-OH brush and 39.5kD-17.7kD BCP, and subsequently wet etched for different intervals.

Time (min)	Measurement 1 (nm)	Measurement 2 (nm)	Measurement 3 (nm)	AVERAGE (nm)
1	-4.331	-3.483	-3.269	-3.694
2	-1.468	-0.506	-0.629	-0.868
3	-0.173	-0.972	-0.854	-0.666
5	0.081	0.373	-0.408	0.287
6	-3.059	-2.162	-1.056	-2.092
7	-0.930	-1.603	3.532	-2.022
10	-3.386	-1.806	-	-2.596

2.2. Studies on Graphene Coated Si Substrates

Graphene substrates were synthesized using CVD technique in the presence of ethyl alcohol. These surfaces, were initially coated with polymer brush, annealed in the vacuum oven at 170°C for lamellar patterns and 190°C for cylindrical patterns. Thus, Si-OH bonds were formed between the surface and the brush. Washing in toluene was carried out to remove excess polymer brush from the surfaces. Then, the surfaces were dried with N₂ flow and coated with PS-*b*-PMMA BCP, annealed on hot plate at the desired temperatures and for the minutes optimized at the previous steps. Microphase separation is obtained in much smaller times on the surfaces which were in direct thermal contact on hot plate.

As a summary, 50% PS brush coated graphene surfaces were annealed at 170°C in a vacuum oven for 2 hours, and after the BCP coating, surfaces were annealed at 240°C on a hot plate. When graphene surfaces were thermally annealed using these optimized parameters of studies made just like on Si/SiO₂ surfaces, obtained AFM images are shown in Figure 4.

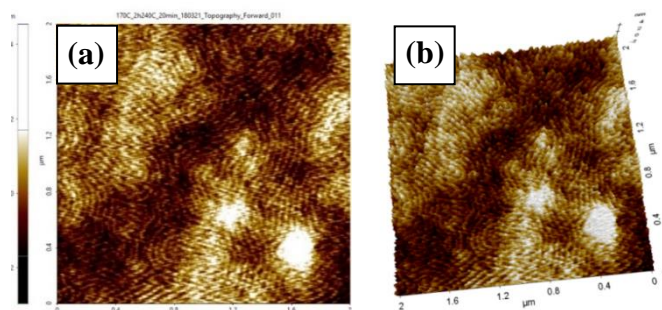


Fig. 4: (a) 1D, (b) 3D AFM topography images of 50% PS brush and 37kD-37kD PS-*b*-PMMA coated graphene surface, after thermal annealing.

After thermal annealing step, graphene substrates coated with both of the polymer brush-BCP pairs were placed in a UV/ozone cleaner for 30 seconds, thus, PS blocks were made more stable in acetic acid due to crosslinking. Later, surfaces that were exposed to wet etching in acetic acid for 4 minutes, were immersed in pure water, and dried in N₂ flow. AFM images displayed in Figure 5 were taken after this process.

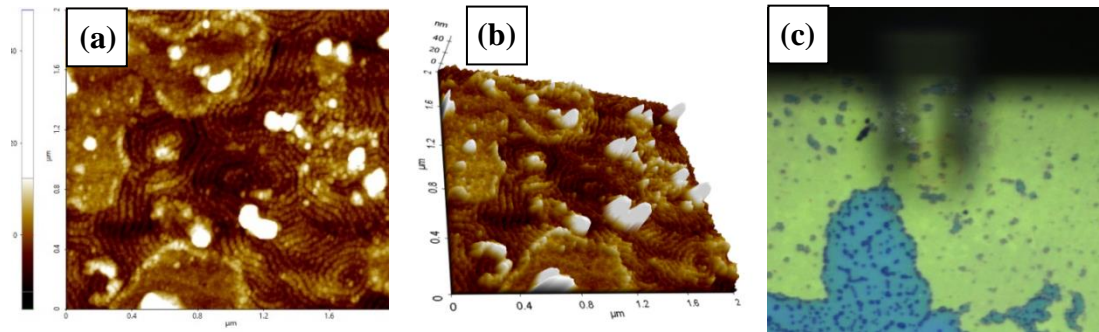


Fig. 5: (a) 1D, (b) 3D AFM topography images of 50% PS brush and 37kD-37kD PS-*b*-PMMA coated graphene surface, after thermal annealing and etching, (c) screenshot of the surface.

In order to include Al atoms into holes formed after the PMMA removal, the substrates were coated with $\text{Al}(\text{NO}_3)_3 \cdot 9\text{H}_2\text{O}$ solution prepared in ethanol, then the substrates were held in UV/ozone for 3 hours to remove polymer and form the metal oxide. Al nanowires which obtained after the metal inclusion technique are shown in Figure 6. These metal nanowires act as hard mask, and play key role in transfer of the obtained microphase pattern to underlayer. At the same time, Al metal, as expressed at the beginning of the studies, have positive effects in increasing the conductivities of the substrates [14], [15], [16].

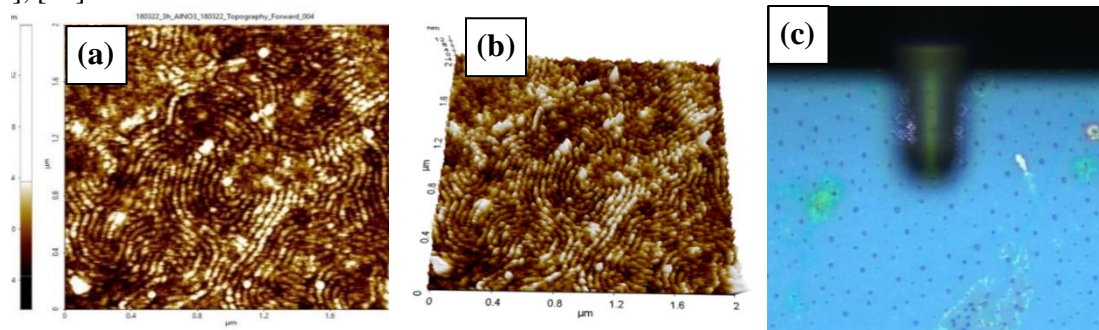


Fig. 6: (a) 1D, (b) 3D AFM topography images of 50% PS brush and 37kD-37kD PS-*b*-PMMA coated graphene surface, after thermal annealing, etching, and metal inclusion, (c) screenshot of the surface.

In order to investigate the effect of UV/ozone treatment time on pattern structures of cross-linked PS segments after etching with acetic acid, interaction time was increased to 40 and 50 seconds. Surfaces prepared for 40 seconds of UV/ozone treatment are shown in Figure 7. Images obtained after 4-minute acetic acid etching are present in Figure 8. Moreover, surface prepared to observe the differences formed when the UV/ozone exposure time was increased up to 50 seconds is given in Figures 9 and 10. Based on these AFM images, it was concluded that as cross-linking time increases, solubility of PS blocks decrease and microphase separations are better on surfaces which were exposed to UV/ozone for 30 seconds.

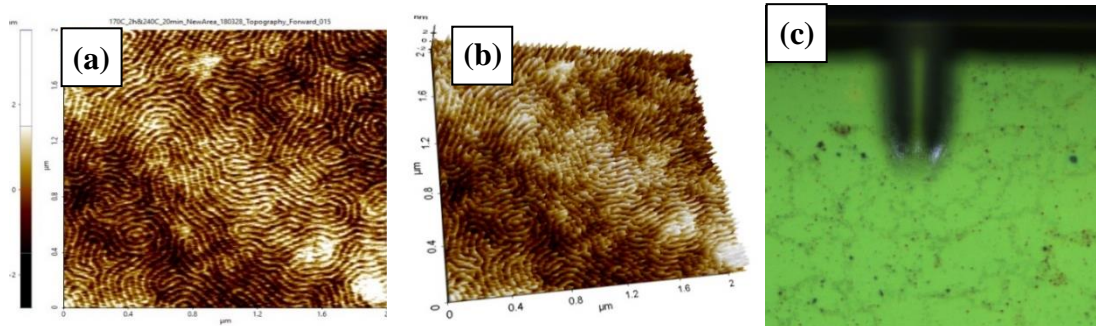


Fig. 7: (a) 1D, (b) 3D AFM topography images of 50% PS brush and 37kD-37kD PS-*b*-PMMA coated graphene surface after thermal annealing, (c) screenshot of the surface. (These surfaces were prepared in order to be exposed to UV/O₃ for 40 seconds.)

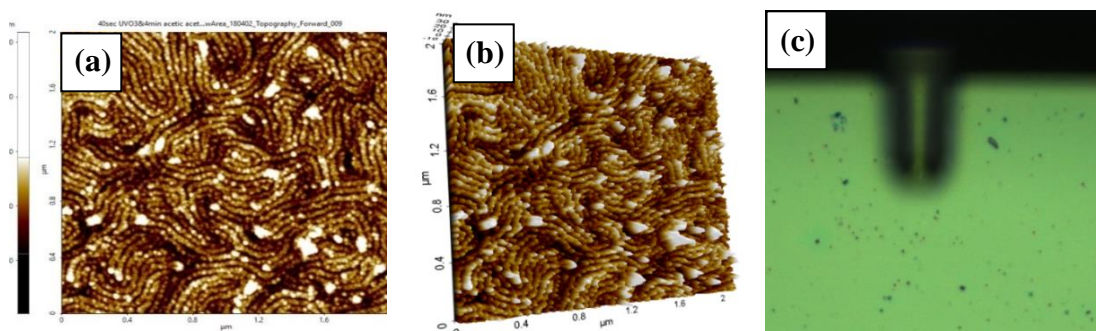


Fig. 8: (a) 1D, (b) 3D AFM topography images of 50% PS brush and 37kD-37kD PS-*b*-PMMA coated graphene surface after thermal annealing, 40-second UV/O₃ treatment and 4-minute acetic acid etching (c) screenshot of the surface.

AFM images present in Figure 9 show the surfaces treated in UV/ozone for 50 seconds. However after 40 seconds of interaction on the surfaces, only 10 second-extra treatment made pretty hard to take the images. Another reason acting on this situation is the possibility of degradation which could occur on the graphene surfaces.

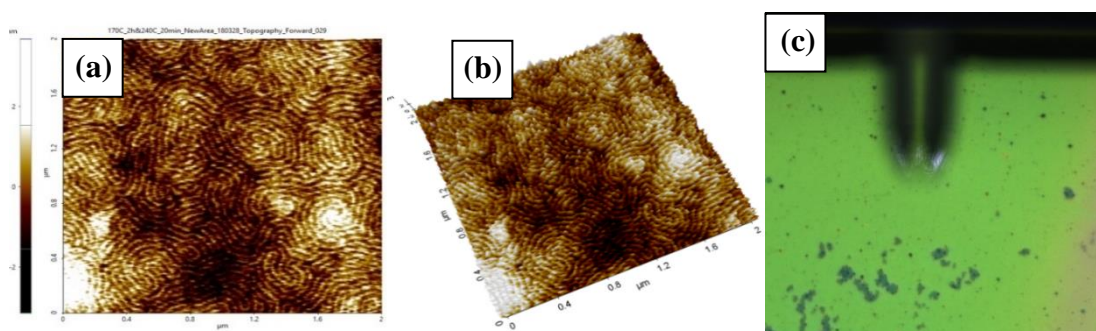


Fig. 9: (a) 1D, (b) 3D AFM topography images of 50% PS brush and 37kD-37kD PS-*b*-PMMA coated graphene surface after thermal annealing, (c) screenshot of the surface. (These surfaces were prepared in order to be exposed to UV/O₃ for 50 seconds.)

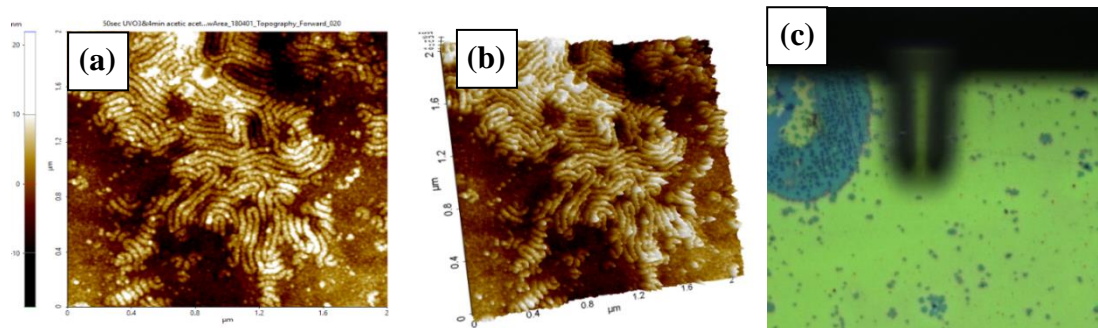


Fig. 10: (a) 1D, (b) 3D AFM topography images of 50% PS brush and 37kD-37kD PS-*b*-PMMA coated graphene surface after thermal annealing, 50-second UV/O₃ treatment and 4-minute acetic acid etching (c) screenshot of the surface.

50% PS brush and 37kD-37kD PS-*b*-PMMA coated graphene surface on which microphase separations and etching steps were applied were characterized as in Figure 11. Height differences caused by the wet treatment can be seen.

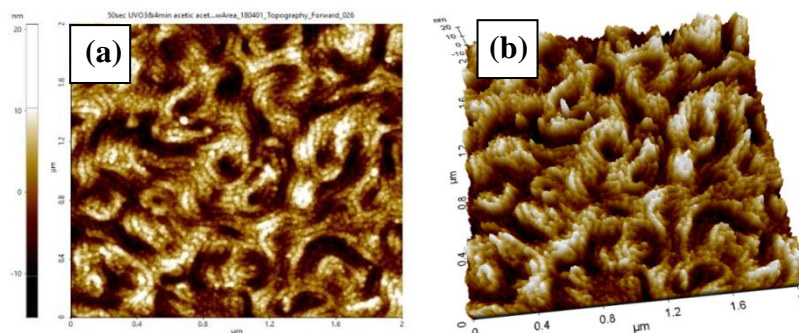


Fig. 11: (a) 1D, (b) 3D AFM topography images of 50% PS brush and 37kD-37kD PS-*b*-PMMA coated graphene surface after thermal annealing, 50-second UV/O₃ treatment and 4-minute acetic acid etching.

Although line patterns were obtained on graphene surfaces being exposed to 50 second UV/ozone, it was observed that chains started to break. Because of this reason, in order to maintain the applicability of ongoing steps, it was decided that optimum interaction time for the surfaces was 30 seconds in UV/ozone and procedure was continued after this arrangement. It was concluded that only 10-second increases in order to maintain 40 and 50 seconds of interactions caused more etching on the surface than the desired amount.

3. Conclusion

Symmetrical PS-*b*-PMMA blocks with 37kD-37kD molecular weight were chosen in order to obtain lamellar BCP patterns, whereas 39.5kD-17.7kD for cylindrical patterns. Si/SiO₂ substrates were coated with the convenient (linear/cylindrical) brush and BCP using spin-coating technique at 3200 rpm for 30 seconds. By the help of thermal annealing, patterning of polymer brush and blocks on the substrates at different temperatures was studied, after the optimized microphase separations were obtained.

Effect of the brush choice on the microphase separation, and the importance of different polymer brush-BCP combinations on the surface patterning were observed. It was concluded that same BCPs gave different microphase patterns using 50% PS, 70% PS and PS-OH brushes, and it was possible to obtain microphase separations with desired geometries when right duos match. Especially when polystyrene brush with hydroxy end group (PS-OH) was used, vertical alignment could be achieved and it was observed that horizontal polymer blocks could be oriented vertically as the result of the selective interaction with polymer brush. This situation can be expressed with one of the key principles 'Like

dissolves like'. From this point of view, similar structures on polymer brush and on block copolymers interact with each other and thus, arrangements in morphology of the film occurs.

In addition to conventional use of vacuum oven, thanks to annealing process made on hot plate, clear microphase separated images were obtained in much shorter time. This is because of the increase in mobility of the polymer blocks. Microphase separated patterns could be observed by saving both on time and energy.

Prior to the etching step made using acetic acid, UV/ozone technique which decreases solubility of PS in acid by increasing cross linking in the PS structure, was applied for 30-50 seconds and optimum cross-linking time was determined as 30 seconds. Due to the damage caused in polymer chains during elongated times, optimization of the treatment time in UV/ozone is of critical importance in terms of continuity of the process.

Metal salt inclusion technique was applied for the formation of Al nanowires and the hard mask. $\text{Al}(\text{NO}_3)_3 \cdot 9(\text{H}_2\text{O})$ solutions prepared in ethanol were spin-coated on substrates which were microphase-separated and etched using acetic acid post cross-linking, afterwards surfaces were held in UV/ozone system for 3 hours. At this step, space formed by PMMA blocks was filled by aluminium and Al nanowires were obtained. These nanowires both act as hard mask and enable the electrical conductivity on the substrate.

After process parameters were optimized on Si/SiO₂ substrates, same steps were repeated on graphene coated substrates.

Graphene surfaces on which Al nanowires formed are ready to be used for subsequent pattern transfer.

Acknowledgements

H.Y. and M.E. acknowledge financial support from Scientific&Technological Research Council of Turkey (TUBITAK) (Project No 114Z934) and Selcuk University Coordinatorship of Scientific Research Projects (SU-BAP) (Project No 17101011). The authors would like to thank Emre Çıtak (Selcuk University) for supplying graphene coated Si substrates.

References

- [1] G. E. Moore, "Cramming more components onto integrated circuits," *Electronics*, pp. 114-117, 1965.
- [2] M. A. Morris, "Directed self-assembly of block copolymers for nanocircuitry fabrication," *Microelectronic Engineering*, vol. 132, pp. 207-217, 2015.
- [3] I. Julie N. L. Albert and Thomas H. Epps, "Self-assembly of block copolymer thin films," *Materials Today*, vol. 13, no. 6, pp. 24-33, 2010.
- [4] I. W. Hamley, "Ordering in thin films of block copolymers: Fundamentals to potential applications," *Progress in Polymer Science*, vol. 34, no. 11, pp. 1161-1210, 2009.
- [5] C. Cummins and M. A. Morris, "Using block copolymers as infiltration sites for development of future nanoelectronic devices: Achievements, barriers, and opportunities," *Microelectronic Engineering*, vol. 195, pp. 74-85, 2018.
- [6] S. Ji, L. Wan, C.-C. Liu, and P. F. Nealey, "Directed self-assembly of block copolymers on chemical patterns: A platform for nanofabrication," *Progress in Polymer Science*, vol. 54-55, pp. 76-127, 2016.
- [7] Y. Zhu *et al.*, "Graphene and graphene oxide: synthesis, properties, and applications," *Adv Mater*, vol. 22, no. 35, pp. 3906-24, 2010.
- [8] O. C. Compton and S. T. Nguyen, "Graphene oxide, highly reduced graphene oxide, and graphene: versatile building blocks for carbon-based materials," *Small*, vol. 6, no. 6, pp. 711-23, 2010.
- [9] A. K. Geim and K. S. Novoselov, "The rise of graphene," *nature materials*, vol. 6, pp. 183-191, 2007.
- [10] S. Park, J. M. Yun, U. N. Maiti, H. S. Moon, H. M. Jin, and S. O. Kim, "Device-oriented graphene nanopatterning by mussel-inspired directed block copolymer self-assembly," *Nanotechnology*, vol. 25, no. 1, p. 014008, 2014.
- [11] T. H. Chang *et al.*, "Directed self-assembly of block copolymer films on atomically-thin graphene chemical patterns," *Sci Rep*, vol. 6, p. 31407, 2016.

- [12] P. Ni, " Band gap of graphene nanoribbons calculated using Huckel molecular orbital theory," *IJEAS*, vol. 2, no. 3, pp. 25-27, 2015.
- [13] C. Cummins, T. Ghoshal, J. D. Holmes, and M. A. Morris, "Strategies for Inorganic Incorporation using Neat Block Copolymer Thin Films for Etch Mask Function and Nanotechnological Application," *Adv Mater*, vol. 28, no. 27, pp. 5586-618, 2016.
- [14] O. T. Özkan and A. J. Moulson, "The electrical conductivity of single-crystal and polycrystalline aluminium oxide," *J. Phys. D: Appl. Phys.*, vol. 3, pp. 983-987, 1970.
- [15] Y. T. Lee and R. M. More, "An electron conductivity model for dense plasmas," *Physics of Fluids*, vol. 27, no. 5, p. 1273, 1984.
- [16] Y. Wan *et al.*, "Conductive and Stable Magnesium Oxide Electron-Selective Contacts for Efficient Silicon Solar Cells," *Advanced Energy Materials*, vol. 7, no. 5, p. 1601863, 2017.